

Templated display of biomolecules and inorganic nanoparticles by metal ion-induced peptide nanofibers†

Byoung-Chul Lee and Ronald N. Zuckermann*

Received (in Austin, TX, USA) 1st December 2009, Accepted 19th January 2010

First published as an Advance Article on the web 3rd February 2010

DOI: 10.1039/b925395e

We functionalized peptide nanofibers to provide a nano-scale template for the display of biomolecules and inorganic nanoparticles using metal ion coordination. Nanofibers assembled only in the presence of certain divalent metal ions, and could be readily dissolved by a metal-chelating reagent, EDTA.

The advancement of modern synthetic chemistry has raised our capability to engineer nanostructures for the efficient display of functional molecules on the nanometre scale, and utilize them for various applications in molecular recognition, catalysis and electronics. For these purposes, organic nanostructures are of great interest due to their ease of functional modification and display. Organic nanostructures of different size and shape have been developed using molecular self-assembly in aqueous solution, ranging from one-dimensional nanofibers and tubes to two-dimensional layers and three-dimensional hydrogels.^{1–4}

Nanofibers derived by the self-assembly of peptides and proteins are of particular interest and found utility as nano-templates for a variety of materials applications because of their strong mechanical properties.⁵ Detailed structural analysis has shown that the core structural motif of the fibers is due to 5 to 10 amino acids.^{1,6–8} The extended β -sheet conformation of these peptides allows individual peptide chains to stack against each other through intermolecular backbone hydrogen bonds.⁷ These cross β -sheets bundle together to form fibrillar structures with a width of 5 to 10 nm.¹ Peptide nanofibers have provided excellent templates to order a variety of different materials.^{9–16}

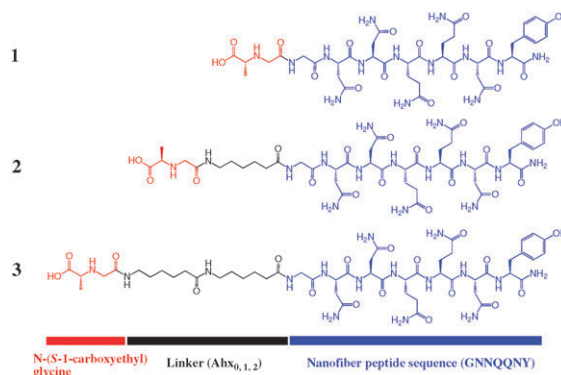
Here, we aim to engineer these peptide nanofibers to provide useful interfaces to both organic and inorganic materials. Toward this goal, we set out to align divalent metal ions along the fibers in order to display proteins and grow metal nanoparticles *via* metal coordination on the surface of the fibers. Among the peptide sequences that form nanofibers, we chose a peptide, Gly-Asn-Asn-Gln-Gln-Asn-Tyr-NH₂ (GNNQQNY-NH₂),⁸ because the side-chains of this peptide have no propensity to coordinate metal ions. In addition, amides from Asn and Gln provide another layer of structural

stabilization for the nanofiber through side-chain hydrogen bonds between peptide chains.⁷ Thus, the fibers are stabilized by hydrogen bonds from both peptide backbones and side-chains.⁷ This particular peptide, GNNQQNY-NH₂, has been studied in detail previously. X-Ray fiber diffraction,⁸ atomic-detailed crystal structure⁷ and computational free energy calculation¹⁷ have been reported with detailed atomic structural information.

In this study, we attached one N-(S-1-carboxyethyl) glycine moiety at the N-terminus of this peptide to provide a partial metal ion coordination site at the nanofiber surface (Scheme 1). In order to separate the functional moiety of this terminal group from the structural body of the peptide, we incorporated either one or two aminohexanoic acid linkers (compounds **2** or **3**, respectively).

In order to understand how the fiber assembly is influenced by divalent metal ions, we measured the fiber formation kinetics in the presence of various metal ions. Using a 96-well plate reader, we recorded the absorbance at 450 nm as an indication of light scattering caused by fibrous aggregation.⁸ As shown in Fig. 1, aggregation occurs only in the presence of Cu(II), Co(II), Zn(II), Ni(II) and Mn(II), for compounds **2** and **3** that have one and two flexible linkers, respectively. In all of these cases, nanofiber formation was confirmed by scanning electron microscopy, as described below (Fig. 2 and ESI†). There was no indication of aggregation in compound **1** even in the presence of metal ions (Fig. 1a). Co(II) increased the absorbance slightly in compound **1**, but well-defined nanostructures were not observed by scanning electron microscopy.

The fibers formed over several hours in the presence of metal ions for compound **2** and **3** (Fig. 1). Fiber formation was metal-dependent, as there was no aggregation in the absence of metal ions on this time scale of 48 hours. It is likely that the



Scheme 1 The chemical structure of peptides with N-terminal N-(S-1-carboxyethyl) glycine moiety used in our study.

Biological Nanostructures Facility, The Molecular Foundry, Lawrence Berkeley National Laboratory, 1 Cyclotron Rd., Berkeley, CA 94720, USA. E-mail: rnzuckermann@lbl.gov; Fax: +1 510-495-2376; Tel: +1 510-486-7091

† Electronic supplementary information (ESI) available: Materials and methods, scanning electron microscopy images, X-ray power diffraction data, binding of mCherry to the metal-ion induced fibers, binding of mCherry (lacking his₆ tag) to the fibers, size distribution of Cu and Ni nanoparticles, and high-resolution TEM images of the metal nanoparticles. See DOI: 10.1039/b925395e

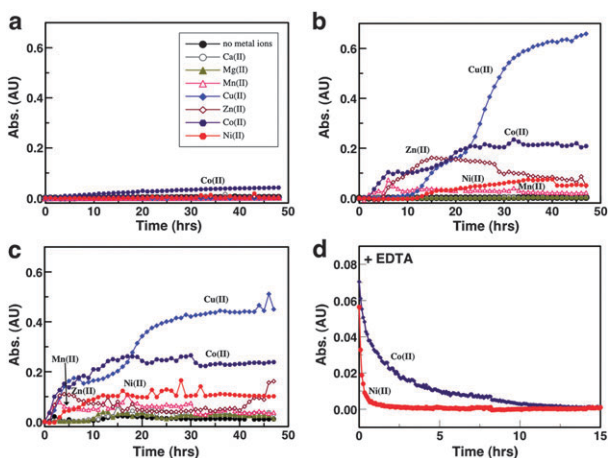


Fig. 1 Kinetics of the fiber assembly (a–c) and disassembly (d). The final 0.5 mM of each compound (a) **1**, (b) **2**, and (c) **3** was used for the fiber formation in the presence of 5 mM of metal ions. (d) 100 mM of EDTA were added to the metal ion-induced fibers assembled from the compound **3** with a ratio of 1 : 1 (v/v).

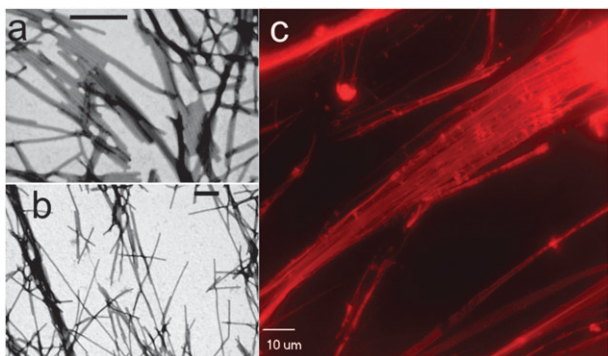


Fig. 2 TM-SEM images of (a) Cu(II)- and (b) Ni(II)-induced fibers assembled from compound **3** with 200 nm scale bar, and (c) fluorescence microscopy image of his₆-tagged mCherry binding to Ni(II)-induced fibers assembled from compound **3**. The excess metal ions were removed by dialysis before adding his₆-tagged mCherry.

carboxyl group of the *N*-(*S*-1-carboxyethyl) glycine moiety that we introduced at the *N*-terminus of peptide chain will be negatively charged at pH 7.5, and thus prevent fiber formation due to charge–charge repulsion between adjacent peptide chains.

N-methyl glycine, which is a simple analog of the *N*-terminal *N*-(*S*-1-carboxyethyl) glycine group appended to our peptides, forms 1 : 1 complexes with metal ions with quite low stability constants. For example, the log *K* for complexes of *N*-methyl glycine and Cu(II)-, Zn(II)-, Ni(II)- and Co(II)- are 4.6, 4.3, 5.4 and 4.3 respectively.^{18–20} In the context of the formed fiber, however, these groups are positioned in close proximity to one another to create higher-affinity multivalent metal binding sites. Evidence for this is that the fibers do not disassemble and maintain the bound metal ions upon prolonged dialysis against buffer containing no metal ion. In addition, the Co(II)- and Ni(II)-induced fibers were dissolved upon the addition of 20 eq. of the strong metal-chelating agent, EDTA (Fig. 1d), yielding the fiber dissolution rate constants of $1.0 \times 10^{-4} \text{ s}^{-1}$ and $1.6 \times 10^{-3} \text{ s}^{-1}$, respectively. Other metal-induced fibers (Cu, Zn and Mn) were readily

dissolved by the EDTA within the first 20 min of mixing. This variation in the EDTA-induced dissolution rates suggests that the metal dissociation itself is the rate-limiting step of fiber dissolution, since the peptide–peptide association is too weak for fibers to exist in the absence of metal ions. These results indicate that high-affinity metal binding sites were created by the *N*-(*S*-1-carboxyethyl) glycine displayed on the fibers, especially for Co(II)- and Ni(II)-induced fibers. Thus, the metal ions increased the affinity of peptide self-association, which concomitantly created the high-affinity metal binding sites.

The kinetics of fiber formation were faster by ~5 hours for the sequence with two linkers (compound **3**) than with one linker (compound **2**), especially for Cu(II)- and Co(II)-induced fibers. It is likely that the longer flexible linker either allowed structural optimization for the multivalent metal ion–carboxyl coordination, or the increase in hydrophobicity of the additional methylene groups in the linker increased the propensity to form the fibers.

The degree of final aggregation in Fig. 1 follows the order, Cu(II) > Co(II) > Zn(II) > Ni(II) ≈ Mn(II). This order of preference matches up with the Irving–Williams series that describes the binding preference of divalent first-row transition-metal ions for any given ligands including carboxyl groups.²¹ Thus, it is likely that the decrease in ionic radii for the metal–ligand bonds is primarily responsible for the higher degree of fiber formation.

We characterized the size and shape of the metal-induced fibers using transmission mode-scanning electron microscopy (TM-SEM) at 30 kV after negative staining with uranyl acetate. The width of the fibers was well defined at 11 ± 1 nm from both compound **2** (ESI⁺) and **3** (Fig. 2 and ESI⁺). The length varied from a few tens of nanometres to a few microns. We identified a 4.8 Å molecular spacing from the powder X-ray diffraction (ESI⁺), which is a signature of the regular stacking of each β-strand.^{7,8}

Since we were able to align many multivalent metal ions along the fibers, we further engineered the fibers for structural interfaces with proteins and inorganic materials. As our first test for the interface, we chose the binding of a his₆-tagged protein to the fibers by metal coordination. Co(II)- and Ni(II)-carboxyl coordination can accommodate additional ligands from histidines in proteins. This is analogous to Ni–NTA resins commonly used for purifying his₆-tagged proteins.²² In order to test this hypothesis, we used a red fluorescent protein (RFP), mCherry, to visualize the fibers with fluorescence microscopy. As shown in Fig. 2c and ESI⁺, the fibers induced by Co(II) and Ni(II) ions were decorated with the mCherry protein, indicating that the proteins are aligned along the fibers. To confirm that the mCherry proteins bind to the fibers through the his₆-tag, we used the same mCherry without the his₆-tag. In this case, there was no indication of binding for this protein to the fibers (ESI⁺). Thus, the his₆-tag was able to mediate the binding of proteins to the fibers by specific metal coordination chemistry.

In order to nucleate the growth of metal nanoparticles along the fibers, we hypothesized that metal ions could be reduced along the fibers and initiate the growth of metal nanoparticles by the addition of a reducing reagent. Due to the high-affinity binding of metal ions to the fibers, the growth of metal

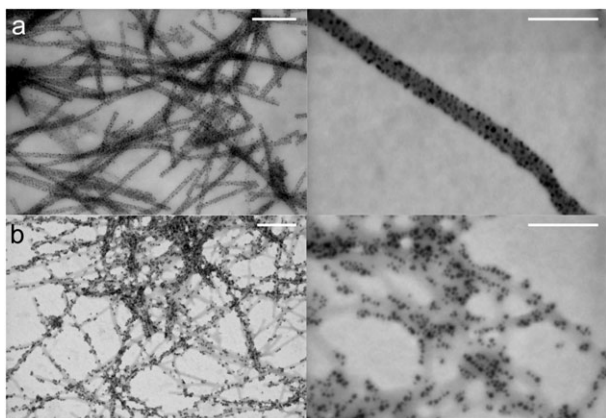


Fig. 3 Growth of (a) Cu and (b) Ni nanoparticles on the fibers assembled from the compound **3** with 200 nm (left panel) and 100 nm (right panel) scale bars.

nanoparticles might be limited to the site of the metal binding along the fibers, and subsequently yield a well-defined size and shape. As expected, Cu and Ni nanoparticles were grown from the fibers that assembled from the compound **3** after the addition of a reducing reagent, sodium borohydride (Fig. 3 and ESI[†]). The average diameters obtained from the image analysis with TM-SEM images are 4.0 ± 1.9 nm and 4.1 ± 1.8 nm for the Cu and Ni nanoparticles, respectively. Other metals were grown, but with more continuous deposition of metal along the fibers. In order to probe the crystallinity of the metal nanoparticles, high-resolution TEM (HRTEM) at 200 kV was carried out for both Cu and Ni nanoparticles. The Cu nanoparticles clearly showed a crystalline phase, but the Ni nanoparticles did not show a clear lattice fringe, but did contain domains of crystal lattice (ESI[†]).

Transition metal nanoparticles such as Cu and Ni have been used for catalysts, for example, growing carbon nanotubes.^{23,24} Our fibers with a regular linear array of Cu or Ni nanoparticles would have the potential to grow regularly aligned carbon nanotubes, and many other applications for optics, electronics, antifouling agents, etc.²⁵

In summary, we developed a reversible molecular fiber assembly. A terminal N-(S-l-carboxyethyl) glycine group prevented the growth of the fibers in the absence of metal ions. However, nanofibers assembled from the modified peptides only in the presence of certain divalent metal ions, creating high-affinity multivalent metal binding sites along the fiber axis. Nanofibers could be readily dissolved by the strong metal-chelating reagent, EDTA. This reversible feature of peptide nanofibers offers a new tool to create nanostructures with precise spatiotemporal control. Using metal ion coordination, we were able to align a his₆-tagged protein, and template the growth of metal nanoparticles along the fibers. Thus, our peptide nanofibers provide a nano-scale linear template for the display of biomolecules and inorganic nanoparticles.

We thank Dr Caroline Ajo-Franklin for providing the *Escherichia coli* strain that overexpress mCherry, Dr Virginia Altoe for operating the HRTEM, and Amanda Marciel for powder X-ray diffraction. We also thank Michael Connolly for valuable comments and assistance. This work was performed at the Molecular Foundry, Lawrence Berkeley National Laboratory, and was supported by the Office of Science, Office of Basic Energy Sciences, of the U.S. Department of Energy under Contract No. DE-AC02-05CH11231.

Notes and references

- 1 I. W. Hamley, *Angew. Chem., Int. Ed.*, 2007, **46**, 8128–8147.
- 2 T. Shimizu, M. Masuda and H. Minamikawa, *Chem. Rev.*, 2005, **105**, 1401–1443.
- 3 S. G. Zhang, *Nat. Biotechnol.*, 2003, **21**, 1171–1178.
- 4 H. Rapaport, *Supramol. Chem.*, 2006, **18**, 445–454.
- 5 T. P. Knowles, A. W. Fitzpatrick, S. Meehan, H. R. Mott, M. Vendruscolo, C. M. Dobson and M. E. Welland, *Science*, 2007, **318**, 1900–1903.
- 6 M. R. Sawaya, S. Sambashivan, R. Nelson, M. I. Ivanova, S. A. Sievers, M. I. Apostol, M. J. Thompson, M. Balbirnie, J. J. W. Wiltzius, H. T. McFarlane, A. O. Madsen, C. Riekel and D. Eisenberg, *Nature*, 2007, **447**, 453–457.
- 7 R. Nelson, M. R. Sawaya, M. Balbirnie, A. O. Madsen, C. Riekel, R. Grothe and D. Eisenberg, *Nature*, 2005, **435**, 773–778.
- 8 M. Balbirnie, R. Grothe and D. S. Eisenberg, *Proc. Natl. Acad. Sci. U. S. A.*, 2001, **98**, 2375–2380.
- 9 B. J. Pepe-Mooney and R. Fairman, *Curr. Opin. Struct. Biol.*, 2009, **19**, 483–494.
- 10 L. C. Palmer, C. J. Newcomb, S. R. Kaltz, E. D. Spoerke and S. I. Stupp, *Chem. Rev.*, 2008, **108**, 4754–4783.
- 11 T. Scheibel, R. Parthasarathy, G. Sawicki, X. M. Lin, H. Jaeger and S. L. Lindquist, *Proc. Natl. Acad. Sci. U. S. A.*, 2003, **100**, 4527–4532.
- 12 E. Kasotakis, E. Mossou, L. Adler-Abramovich, E. P. Mitchell, V. T. Forsyth, E. Gazit and A. Mitraki, *Biopolymers*, 2009, **92**, 164–172.
- 13 Y. B. Lim, E. Lee and M. Lee, *Angew. Chem., Int. Ed.*, 2007, **46**, 3475–3478.
- 14 V. Dinca, E. Kasotakis, J. Catherine, A. Mourka, A. Ranella, A. Ovsianikov, B. N. Chichkov, M. Farsari, A. Mitraki and C. Fotakis, *Nano Lett.*, 2008, **8**, 538–543.
- 15 F. Gelain, A. Horii and S. G. Zhang, *Macromol. Biosci.*, 2007, **7**, 544–551.
- 16 S. M. Pilkington, S. J. Roberts, S. J. Meade and J. A. Gerrard, *Biotechnol. Prog.*, DOI: 10.1002/btpr.309.
- 17 B. Strodel, C. S. Whittleston and D. J. Wales, *J. Am. Chem. Soc.*, 2007, **129**, 16005–16014.
- 18 S. P. Datta, R. Leberman and B. R. Rabin, *Trans. Faraday Soc.*, 1959, **55**, 1982–1987.
- 19 R. M. Izatt, J. J. Christensen and V. Kothari, *Inorg. Chem.*, 1964, **3**, 1565–1567.
- 20 D. L. Leussing and E. M. Hanna, *J. Am. Chem. Soc.*, 1966, **88**, 693–696.
- 21 H. Irving and R. J. P. Williams, *J. Chem. Soc.*, 1953, 3192–3210.
- 22 J. Crowe, H. Dobeli, R. Gentz, E. Hochuli, D. Stuber and K. Henco, *Methods Mol. Biol.*, 1994, **31**, 371–387.
- 23 W. W. Zhou, Z. Y. Han, J. Y. Wang, Y. Zhang, Z. Jin, X. Sun, Y. W. Zhang, C. H. Yan and Y. Li, *Nano Lett.*, 2006, **6**, 2987–2990.
- 24 C. P. Deck and K. Vecchio, *Carbon*, 2006, **44**, 267–275.
- 25 K. C. Anyaogu, A. V. Fedorov and D. C. Neckers, *Langmuir*, 2008, **24**, 4340–4346.